V.V. VAINBERG, A.S. PYLYPCHUK, V.N. POROSHIN, O.G. SARBEY

Institute of Physics, Nat. Acad. of Sci. of Ukraine
*(46, Nauky Ave., Kyiv 03028, Ukraine)*

# EFFECTS OF THE REAL-SPACE TRANSFER OF CHARGE CARRIERS IN THE *n*-AlGaAs/GaAs HETEROSTRUCTURES WITH THE DELTA-LAYERS OF IMPURITY IN THE BARRIERS

PACS 72.20.Fr, 72.80.Ey, 73.21.Fg, 73.63.Hs, 81.07.St

*The results of investigations of the electric and magnetic transport phenomena of charge carriers in the heterostructures with quantum wells and impurity delta-layers in adjacent barriers are reviewed and analyzed. The positive magnetoresistance observed at low temperatures ($T < 20$ K) and the dependence of the charge carrier mobility on the impurity concentration in the delta layers are related to the transport of carriers via two parallel channels with different mobilities, which are the channels formed by the structural and delta-layer quantum wells. The non-linear dependence of the current on the applied electric field strength is explained by the field-induced redistribution of charge carriers between these channels.*

*K e y w o r d s:* heterostructures, quantum wells, lateral conduction, magnetoresistance, delta doping.

## 1. Introduction

The increase of the average kinetic energy of the free charge carriers in the semiconductor heterostructures due to heating them by the applied lateral (directed along the layers) electric field or due to increasing temperature leads to redistribution of carriers among adjacent layers [1, 2]. The difference of the mobilities in layers is usually achieved due to the selective doping, which leads to the additional scattering by impurities, or different thicknesses of layers, which determines the roughness scattering intensity at heterointerfaces.

The phenomenon of the real-space transfer of charge carriers was observed in various kinds of heterostructures: the single-kind quantum wells (QW) with selectively doped barriers; the non-doped tunnel-coupled quantum wells (TCQW) of different widths; the tunnel-coupled quantum wells with doping in one of them; and the quantum well tunnel-coupled with a fragment of the short-period superlattice (see, e.g., [3–6]). A great number of effects caused by the real-space transfer was found: the current saturation or negative differential conductivity (NDC) (see, e.g., [7]), variations of the absorption coefficient and the refractive index in the course of intersubband transitions of carriers [4], the decrease of the emission intensity by hot carriers [8], *etc.* A lot of them are useful for applied purposes. Mainly this is NDC which is used for the generation of HF current oscillations.

The present paper is devoted to reviewing our investigations of the transport phenomena of charge carriers in the electric and magnetic fields in the heterostructures, which contain the impurity delta-like layers in the barriers nearby to the edges of quantum wells, and the impurity concentration has such a value that the impurity well for charge carriers is formed, which is tunnel-coupled with the main (structural) QW. A number of their properties is discussed, which gives the evidence of the efficient redistribution of charge carriers between the structural and impurity quantum wells.

The investigations have been carried out with the samples of the $Al_xGa_{1-x}As/GaAs/Al_xGa_{1-x}As$ heterostructures, $x = 0.15$. The structures were grown by the MOVPE method on the semiinsulating substrates of GaAs (100) in the N.-Novgorod State University (Russia). They consist of 10 periods (repetitions), each of which containing the 80 Å wide quantum well and is doped in the barrier by the delta-layer of the Si donor impurity with concentration in the range from $4 \times 10^{11}$ cm$^{-2}$ to $2.5 \times 10^{12}$ cm$^{-2}$. The impurity layer has the effective width of ∼20 Å and is formed at the 100 Å distance from the well edge. The

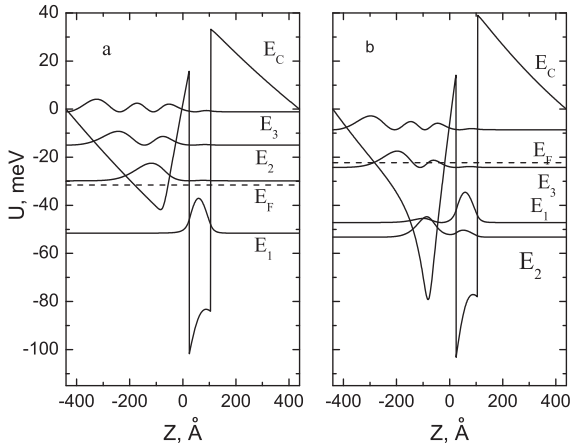


***Fig. 1.*** Energy band spectra of the structures with 2 impurity concentrations, $N_{\rm Si}$: $4.75\times10^{11}$ cm$^{-2}$ ($a$) and $1.4\times10^{12}$ cm$^{-2}$ ($b$). $E_{\rm C}$ – the conduction band bottom profile, $E_1$, $E_2$, $E_3$ – size quantization levels and squared envelope wave functions of electrons, $E_{\rm F}$ – the Fermi level

background impurity concentration all over the structure is about $5 \times 10^{15}$ cm$^{-3}$.

## 2. The Potential Profile of the Conduction Band Bottom and Electron Energy Spectrum in the Structures under Study

Calculations of the conduction band bottom potential profile, energy spectrum, and wave functions of free electrons in the structures under study were carried out by the numerical method of the self-consistent solution of the system of the one-dimensional (along the structure growth direction) Schrödinger and Poisson equations with the electroneutrality condition for a one period of the structure. In this approach, the structure is considered as an infinite chain of identical periods with cyclic boundary conditions. The procedure of calculations is described in detail elsewhere [9].

Shown in Fig. 1 are the results of calculations for two concentrations of the doping impurity at $T = 4.2$ K.

Figure 1 shows that, in the plane of the $\delta$-doping layer, a V-shaped impurity potential well, which arises as a consequence of the Coulomb interaction of free electrons and impurity ions, exists. The distance between the impurity and structural wells is about the Bohr radius of electrons at the impurity ions. Therefore, the wells are tunnel-coupled, and the spectrum of free electrons is the system of size quantization subbands, which is common for both wells.

In the case of weakly doped structures ($N_{\rm Si} \leq 6.5\times$ $\times10^{11}$ cm$^{-2}$), the impurity QW is shallower than the structural one. The Fermi level is below the second size quantization subband. Therefore, at the temperature under consideration, all the carriers are in the first subband and, as is seen from Fig. 1, they are located within the structural QW. With increasing the doping concentration, the impurity well is deepening. At $N_{\rm Si} = 1.4 \times 10^{12}$ cm$^{-2}$, its depth becomes close to that of the structural one. Along with that, the electron densities become approximately equal in both coupled wells. Figure 2, $a$ depicts the calculated dependence of the carrier concentrations in both wells on the doping level of the structure at $T = 4.2$ K. Figure 2, $b$ depicts the dependences of the concentration in both wells on the temperature for two impurity concentrations.

One can see from Fig. 2, $a$ that increasing the doping concentration above $N_{\rm Si} = 5 \times 10^{11}$ cm$^{-2}$ leads only to increasing the electron concentration in the impurity QW, while the concentration in the structural well remains about constant. It is caused by the fact that, at such carrier concentrations, the Fermi energy exceeds the bottom of the second size quantization subband. As the temperature increases, the electrons are redistributed between coupled wells (Fig. 2, $b$).

## 3. Lateral Transport of Electrons under Weak Electric Fields

Let us consider now features of the charge carrier lateral transport in such structures under a weak (nonheating) electric field, which are caused by the possibility for carriers in two coupled wells to participate in it. Depicted in Fig. 3 are the electron mobility vs temperature dependences in the structures with different $\delta$-doping levels. These dependences are derived from the experimental temperature dependences of the Hall coefficient and resistivity as $\mu_{\rm Hall} = R_{\rm Hall}/\rho$.

One can see from Fig. 3 that the measured mobility of electrons in the heterostructures with different doping levels at high temperatures is almost the same for all samples and is about 3000 cm$^2$/V·s. In this case, the conduction goes both via the structural and impurity wells, the dominating scattering mechanism being the scattering by optical phonons. As a consequence, the measured common mobility of electrons

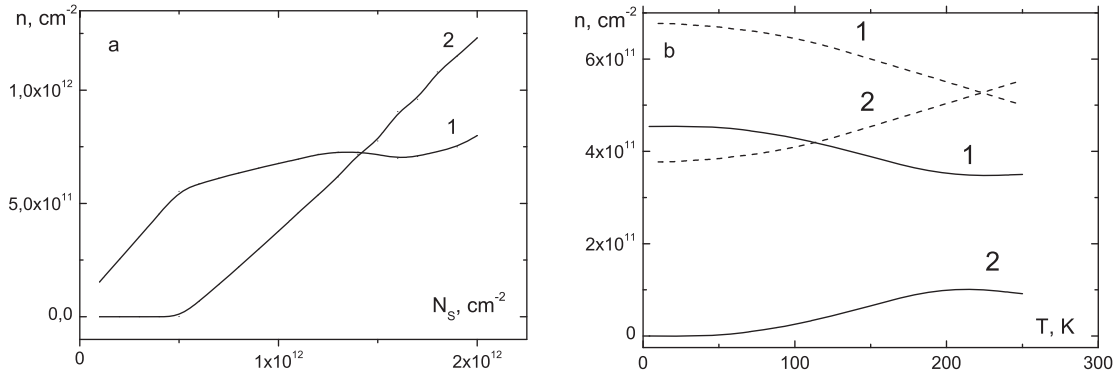


***Fig. 2.*** Dependences of the electron concentrations in the structural (*1*) and impurity (*2*) quantum wells on the doping level at $T = 4.2$ K (*a*) and on the temperature (*b*) for $N_{\rm Si} = 4.7 \times 10^{11}$ cm$^{-2}$ (solid lines) and $N_{\rm Si} = 1.1 \times 10^{12}$ cm$^{-2}$ (dash lines)

is in fact independent of the doping concentration. At low temperatures ($T \leq 20$ K), the measured mobility begins to decrease strongly with increasing the doping concentration above $\sim 5 \times 10^{11}$ cm$^{-2}$. This is caused by an increase of the charge carrier concentration in the impurity QW (Fig. 2) where their mobility is considerably less as compared to the structural wells due to the scattering by impurities. One should notice that, with increasing the total concentration of charge carriers (impurities), the Fermi level and the average energy of carriers increase. Hence, the scattering of carriers by the ionized impurity becomes weaker. This explains a slower decrease of the mobility with growing the concentration observed for the most heavily doped structures.

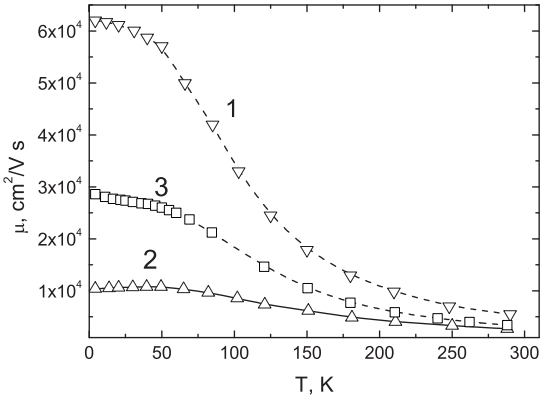


***Fig. 3.*** Temperature dependences of the Hall mobility of electrons in the structures with different doping concentrations $N_{\rm S}$, $10^{11}$ cm$^{-2}$: *1* – 5.4; *2* – 17.5; *3* – 22

## 4. Influence of Conduction via the Impurity δ-layer on the Magneto-Quantum Effects

Conduction via the impurity wells (in addition to the structural QW) causes also features of the magnetotransport of charge carriers in such structures [10]. Shown in Fig. 4 is the dependence of the longitudinal magnetoresistivity on the magnetic field for the structures with the small and large doping concentrations at $T = 4.2$ K. The typical feature for all structures is the negative magnetoresistance in the region of weak (less than 1 T) magnetic fields, which is caused, as is well known, by the effect of weak localization of charge carriers.

With a further increase of the magnetic field, the magnetoresistance of the weakly doped structures tends to saturate, while that of the heavily doped ones changes its sign. At the higher magnetic fields,

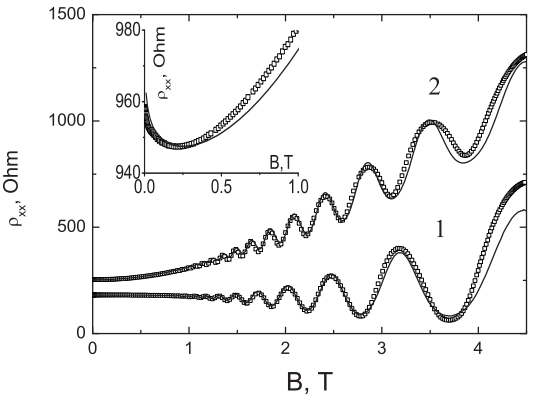


***Fig. 4.*** Dependence of the longitudinal magnetoresistivity on the magnetic field for the structures with $N_{\rm Si} = 5.4 \times$ $\times 10^{11}$ cm$^{-2}$ (*1*) and $17 \times 10^{11}$ cm$^{-2}$ (*2*). Inset: magnetoresistance of the structure with $N_{\rm Si} = 22 \times 10^{11}$ cm$^{-2}$ in the region of weak fields. Lines – the result of calculations [10]

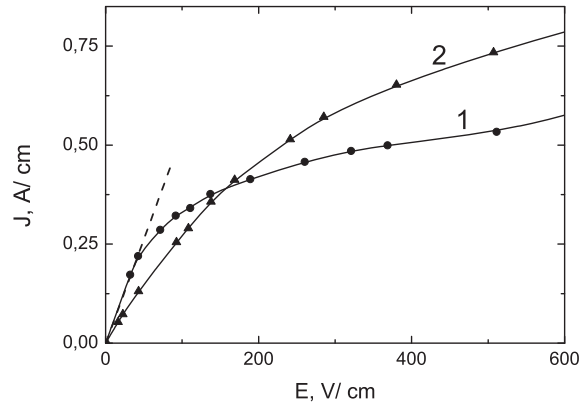


***Fig. 5.*** Current-voltage characteristics of the structure with $N_{\rm Si} = 5.4 \times 10^{11}$ cm$^{-2}$ at $T = 4.2$ K (*1*) and 66 K (*2*)

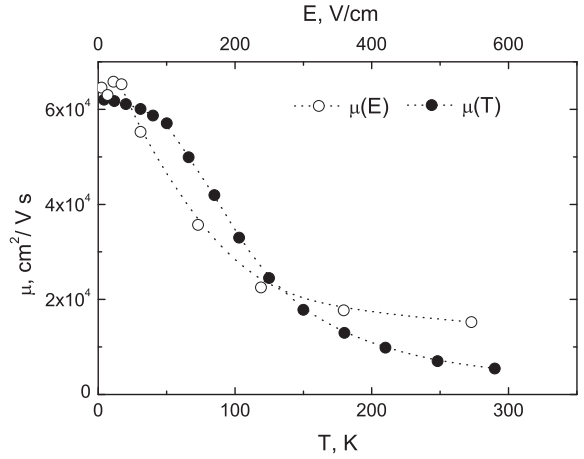


***Fig. 6.*** Dependence of the electron mobility on the temperature under a weak electric field and on the electric field at $T = 4.2$ K for the sample with $N_{\rm Si} = 5.4 \times 10^{11}$ cm$^{-2}$

one also observes the Shubnikov–de Haas oscillations of the magnetoresistance. The FFT analysis of the oscillations shows that the magnetotransport in the weakly doped structures is caused by a single kind of carriers, whose concentration is close to the doping concentration $n = 5.4 \times 10^{11}$ cm$^{-2}$; while, in the heavily doped structures, it is caused by two kinds of carriers with the concentrations $n_1 = 7.55 \times 10^{11}$ cm$^{-2}$ and $n_2 = 1.45 \times 10^{12}$ cm$^{-2}$. This reflects the fact that, in the first case, the free charge carriers fill only the first size quantization subband, and, hence, they move only via the structural wells. While, in the case of large doping concentrations, not only the carriers in the structural wells participate in the magnetotransport, but also the carriers in the impurity wells contribute into it considerably. The presence of two kinds of charge carriers causes also the appearance of the positive magnetoresistance.

The explanation of the magnetoresistance behavior by taking the weak localization into account [11] and the presence of two conduction channels (see, for details, [10]) enabled one to determine the mobility of charge carriers in both kinds of QW. The electron mobility in the impurity QW occurred to be very small: only ∼1000 cm$^2$/V·s for the weakly doped structures and about 700 cm$^2$/V·s for the heavier doped ones. The reason for this, from our point of view, lies in the strong scattering by impurity ions, when the larger portion of charge carriers available in the system is transferred from the impurity to the structural wells.

## 5. Non-Linearity of the Lateral Transport under Strong Electric Fields

Investigations of the strong field lateral electric transport were carried out at temperatures of 4.2 and 66 K and included measurements of the current-voltage characteristics (CVC) and the mobility vs electric field dependences. The measurements were carried out in the pulsed electric fields with a pulse duration of 0.4 $\mu$s and a repetition period of 1 s that enabled us to avoid the Joule heating of samples and the formation of acoustoelectric domains [12]. Shown in Fig. 5 are CVC of the structure with the doping concentration $N_{\rm Si} = 5.4 \times 10^{11}$ cm$^{-2}$ at different temperatures.

One can see from Fig. 5 that, at low temperatures, a strong non-linearity of CVC is observed already at relatively small (∼40 V/cm) fields. At the higher temperature (66 K), the current increases nonlinearly with the electric field. However, the non-linearity is considerably less expressed. At the given doping concentration, the practically all charge carriers at 4.2 K are in the lowest size quantization subband. Thus, they are concentrated in the structural wells. When they are heated-up by the electric field, they transfer into the impurity well, where their mobility considerably decreases due to the impurity scattering. This leads to a strong decrease of the current. At the higher temperatures, the non-linearity is less expressed because the charge carriers initially are in both quantum wells.

The validity of such explanation is confirmed by the mobility vs electric field dependence observed in such structures. This dependence is shown in Fig. 6

for the sample with the doping concentration $N_S = 5.4 \times 10^{11}$ cm$^{-2}$ in which all the electrons at $T = 4.2$ K and weak fields are in the structural well. For the sake of comparison, this picture contains also the mobility vs temperature dependence under a weak electric field.

As one can see from Fig. 6, the mobility in the fields above 40 V/cm begins to decrease sharply, which coincides with a decrease of the CVC slope. However, in the region of strong fields ($E > 300$ V/cm), it changes slowly and is about 15000–20000 cm$^2$/V·s, which exceeds by several times the value in a weak field at the high temperatures (200–300 K), where the mobility is determined by the phonon scattering. In general, the value of mobility decreases with increasing the electric field by more than 3 times. The only reason for such a decrease may be only the transfer of a considerable portion of electrons from the structural well into the impurity one, since the considerable restriction of the hot electron mobility in the structural well due to the scattering by optical phonons is achieved in the fields more than 300 V/cm.

Finally, we should note that the non-linearity of CVC in the studied heterostructures arises at considerably less electric fields than in other kinds of structures with the real-space transfer of hot charge carriers. By optimizing the structure parameters, one can implement the $N$-type CVC which is needed for the generation of HF current oscillations.


1. Z.S. Gribnikov, Fiz. Tekh. Poluprov. **6**, 1380 (1972).
2. Z.S. Gribnikov, K. Hess, and G.A. Kozinovsky, J. Appl. Phys. **77**, 1337 (1995).
3. E.I. Lonskaya and O.A. Ryabushkin, JETP Letters. **82**, 664 (2005).
4. V.L. Zerova, L.E. Vorobjev, D.A. Firsov, and E. Towe, Fiz. Tekh. Poluprov. **41**, 615 (2007) [Semiconductors **41**, 596 (2007)].
5. N. Sawaki, M. Suzuki, Y. Takagaki, H. Goto, I. Akasaki, H. Kano, Y. Tanaka, and M. Hashimoto, Superlatt. and Microstr. **2**, 281 (1986).
6. V.V. Vainberg, A.S. Pylypchuk, N.V. Baidus, and A.A. Biryukov, Low Temper. Phys. **40**, 685 (2014).
7. N. Balkan, B.K. Ridley, and A.J. Vickers, *Negative Differential Resistance and Instabilities in 2-Dimensional Semiconductors* (Plenum Press, New York, 1993).
8. V.Ya. Alyoshkin, A.A. Andronov, A.V. Antonov, N.A. Bekin, V.I. Gavrilenko, D.G. Revin, B.N. Zvonkov, E.R. Linkov, I.G. Malkina, and E.A. Uskova, JETP Letters **64**, 478 (1996).
9. V.V. Vainberg, A.S. Pylypchuk, N.V. Baidus, and B.N. Zvonkov, Semicond. Phys., Quant. Electr. & Optoelectr. **16**, 152 (2013).
10. V.V. Vainberg, A.S. Pylypchuk, V.N. Poroshin, O.G. Sarbey, N.V. Baidus, and A.A. Biryukov, Physica E **60**, 31 (2014).
11. A. Kawabata, J. Phys. Soc. Jap. **53**, 3540 (1984).
12. V.V. Vainberg, Yu.N. Gudenko, P.A. Belevski, M.N. Vinoslavski, V.N. Poroshin, and V.M. Vasetski, Nanosyst., Nanomater., Nanotechn. **4**, 41 (2006).


Received 06.06.14

*В.В. Вайнберг, О.С. Пилипчук,*
*В.М. Порошин, О.Г. Сарбей*

ЕФЕКТИ ПРОСТОРОВОГО ПЕРЕНОСУ НОСІЇВ ЗАРЯДУ В ГЕТЕРОСТРУКТУРАХ $n$-AlGaAs/GaAs З ДЕЛЬТА-ШАРАМИ ДОМІШКИ В БАР'ЄРАХ

Р е з ю м е

Приведено та проаналізовано результати дослідження електричного на магнітного транспорту носіїв заряду в гетероструктурах з квантовими ямами і домішковими дельта-шарами в прилеглих бар'єрах. Додатний магнітоопір і вигляд залежності рухливості носіїв від концентрації домішки в дельта шарах, при низьких температурах ($T < 20$ K), пов'язуються з транспортом носіїв по двох паралельних каналах з різною рухливістю носіїв: структурним і утвореними дельта-шарами домішки квантовим ямам. Нелінійна залежність струму від величини прикладеного електричного поля пояснюється зумовленим полем перерозподілом носіїв між цими каналами.